Giant Pulsations Excited by a Steep Earthward Gradient of Proton Phase Space Density: Arase Observation

Kazuhiro Yamamoto[1] *, Masahito Nosé[1], Satoshi Kasahara[2], Shoichiro Yokota[3], Kunihiro Keika[2], Ayako Matsuoka[4], Mariko Teramoto[5], Kazue Takahashi[6], Satoshi Oimatsu[1], Reiko Nomura[4], Massimo Vellante[7], Balázs Heilig[8], Akiko Fujimoto[9], Yoshimasa Tanaka[10], Manabu Shinohara[11], Iku Shinohara[4], Yoshizumi Miyoshi[5]

Kazuhiro Yamamoto, kazuhiro@kugi.kyoto-u.ac.jp

[1]Graduate School of Science, Kyoto University, Japan

[2]The University of Tokyo, Japan

[3]Osaka University, Japan

[4]Japan Aerospace Exploration Agency, Japan

[5]Nagoya University, Japan

This article has been accepted for publication and undergone full peer review but has not been through the copyediting, typesetting, pagination and proofreading process, which may lead to differences between this version and the Version of Record. Please cite this article as doi: 10.1029/2018GL078293

We present observational evidence of drift resonance between westward propagating odd mode standing ultralow-frequency waves and energetic protons. Compressional ∼13 mHz (Pc4 band) waves and proton flux oscillations at >50 keV were detected at ∼03 hr magnetic local time by the Arase satellite on 15 April 2017. The azimuthal wave number (m number) is estimated to be ~ -50 from ground observations, while the theory of drift resonance gives $m \sim -49$ for odd mode waves and ∼110 keV protons, providing that the drift resonance indeed took place in this event. We also found a steep

[6]The Johns Hopkins University Applied Physics Laboratory, USA

[7]University of L'Aquila, Italy

[8]Mining and Geological Survey of Hungary, Hungary

[9]Kyushu University, Japan

[10]National Institute of Polar Research, Japan

[11]National Institute of Technology, Kagoshima College, Japan

[*]Graduate School of Science, Kyoto University, Kitashirakawaoiwake-cho, Sakyo-ku, Kyoto, 606-8502, Japan

earthward gradient of proton phase space density, which can quantitatively explain the wave excitation. The observed waves show typical features of giant pulsations (Pgs), regarding local time, m number, and flux oscillations. This study, therefore, has great implications to the field line mode structure and excitation mechanism of Pgs.

Keypoints:

- Pc4 ULF waves and proton flux oscillations were observed by Arase and ground magnetometers.
- The azimuthal wave number estimated from ground magnetometers is consistent with the theory of drift resonance.
- The steep gradient of proton phase space density is responsible for the wave excitation.

1. Introduction

Drift resonance or drift-bounce resonance between charged particles and ultralow-frequency (ULF) waves have been drawing attentions for a long time. Since *Southwood et al.* [1969] first proposed the resonance mechanisms, many researchers have considered that westward propagating poloidal Pc4–5 (the frequency range of 1.7–22 mHz) waves with large azimuthal wave number (m number) observed in the inner magnetosphere are excited through drift resonance or drift bounce resonance with the ring current ions. The resonance condition is

$$\omega - m\omega_d = N\omega_b, \tag{1}$$

where ω is a wave angular frequency, m denotes the azimuthal wave number (defined to be positive for eastward propagation), N is an integer that corresponds to mode structure of ULF waves along the field line ($N = 0, \pm 2, ...$ for odd mode and $N = \pm 1, \pm 3, ...$ for even mode), and ω_d and ω_b are drift and bounce angular frequencies, respectively. According to *Southwood et al.* [1969], whether the resonant particles contribute to wave growth or damping depends on the sign of

$$\frac{df}{dW} = \left.\frac{\partial f}{\partial W}\right|_{M_{res},L} + \frac{dL}{dW}\left.\frac{\partial f}{\partial L}\right|_{M_{res},W_{res}}, \tag{2}$$

where f is the phase space density, M_{res} is the magnetic moment of resonant particles, L is the McIlwain's L-shell parameter [*McIlwain*, 1961], and W_{res} is the resonant energy. If $\frac{df}{dW}$ is positive (negative), waves are excited (damped) and particles lose (gain) energy.

Equation (1) gives a constraint among resonant energy, mode structure of ULF waves along the field line, and m number in drift resonance or drift-bounce resonance. Drift-bounce resonance ($N = -1$) between 80–170 keV protons and second harmonic poloidal

waves with $m \sim -100$ was reported by *Takahashi et al.* [1990] and *Min et al.* [2017]. *Takahashi et al.* [2018] also discussed the drift-bounce resonance ($N = 1$) between 1–10 keV protons and second harmonic poloidal waves with $m \sim -200$. *Dai et al.* [2013] showed fundamental poloidal waves with $m \sim -70$ are excited by drift resonance ($N = 0$) with ~ 90 keV protons. These large-m waves are generally observed only by satellites because ionospheric screening effects prevent detection of these waves by ground magnetometers [*Hughes & Southwood*, 1976].

Giant pulsations (Pgs) are another type of ULF waves that are considered to be excited through wave-particle interactions. Pgs generally have large amplitudes with highly monochromatic waveform and are observed by ground magnetometers. The east-west component of the magnetic field amplitude is dominant on the ground, and this indicates that Pgs are related to poloidal waves in the magnetosphere [*Chisham & Orr*, 1991; *Glassmeier*, 1980]. It has been reported that Pgs propagate westward ($m < 0$) and have smaller m number ($|m| = 10 - 40$) [*Takahashi et al.*, 1992; *Chisham et al.*, 1997; *Glassmeier et al.*, 1999; *Motoba et al.*, 2015] than those of the large-m waves ($|m| = 70 - 200$). Ground observations have revealed that Pgs tend to be detected in the morning sector (around 03 MLT) and at $L \sim 6$ during equinoxes or low solar activity [*Sucksdorff*, 1939; *Brekke et al.*, 1987; *Chisham & Orr*, 1994; *Motoba et al.*, 2015]. Although there are a few suggestions that substorm injection and drift velocity dispersion could create the MLT dependence of Pgs [*Glassmeier et al.*, 1999; *Wright et al.*, 2001], the reason of the locality and solar activity dependence has not been fully understood yet. In addition, the oscillation mode of Pgs remains to be determined. Both drift resonance with fundamental waves

and drift-bounce resonance with second harmonic waves are considered as possible mechanisms of excitation of Pgs [*Takahashi et al.*, 1992, 2011; *Chisham & Orr*, 1991; *Wright et al.*, 2001]. Assuming that ∼10 keV protons resonate with second harmonic poloidal waves through drift-bounce resonance, some authors conducted numerical simulations and explained the MLT or solar activity dependence by the change of open/closed orbit of ∼10 keV protons [*Chisham*, 1996; *Ozeke & Mann*, 2001]. However, no satellite observations have provided evidence that ∼10 keV protons excite Pgs. Geosynchronous satellites have observed proton flux oscillations at >95 keV related to Pgs [*Thompson & Kivelson*, 2001; *Motoba et al.*, 2015], and this supports drift resonance with fundamental mode waves. In these observations, however, it was not discussed if Pgs are excited by resonant particles or vice versa, according to equation (2). Because geosynchronous satellites hardly move in the radial direction, it is difficult to evaluate the radial gradient of phase space density, or the second term of the right-hand side of equation (2). Several studies have pointed out that a bump-on-tail structure causes a positive $\frac{\partial f}{\partial W}$ and excites Pgs [*Glassmeier et al.*, 1999; *Wright et al.*, 2001]; however, the relative importance between the first term and the second term of equation (2) has not been discussed yet.

In this study, we report Pc4 ULF waves and proton flux oscillations observed by the Arase satellite [*Miyoshi et al.*, 2018] and ground magnetometers on 15 April 2017. We estimate the radial gradient of the proton phase space density $\left(\frac{\partial f_{H^+}}{\partial L}\right.$, where f_{H^+} is the proton phase space density$\left.\right)$ from the radial motion of Arase to examine the instability condition. We also examine $\frac{\partial f_{H^+}}{\partial L}$ at the apogee using an ion sounding technique [e.g., *Su et al.*, 1977] and find direct evidence of drift resonance driven by the unstable spatial

distribution of f_{H^+}. Finally, implications for the oscillation mode structure and excitation mechanism of Pgs are discussed.

2. Instrumentation

The Arase satellite, whose main objective is exploration of the outer radiation belt, was launched on 20 December 2016 into an elliptical orbit with the apogee of ∼6 R_E and the perigee altitude of $\gtrsim$300 km [*Miyoshi et al.*, 2018]. The satellite is spin stabilized ($\tau_{spin} \sim 8$ sec, where τ_{spin} is the spin period) and equipped with comprehensive sensors for fields and particles. The magnetic field and energetic ion data from Magnetic Field Experiment (MGF) instrument [*Matsuoka et al.*, 2018] and Medium-Energy Particle Experiments - Ion Mass Analyzer (MEP-i) [*Yokota et al.*, 2017] on board the Arase satellite were analyzed in this study. The MEP-i instrument provides three dimensional flux data for H^+, He^{++}, He^+, O^{++}, O^+, and O_2^+ with a time resolution of ∼8 or ∼16 s. The energy range of MEP-i was 5.1–109.6 keV/q before 21 April 2017 and is 9.6–184.2 keV/q afterward. The aperture of MEP-i has 2π-radian field of view (FOV) and ions entering through the aperture are detected by 16 anodes circularly arrayed at 22.5° intervals. Since a normal vector of the 2π-radian FOV plane is almost perpendicular to the spin axis, MEP-i can scan 4π sr due to the Arase's spin motion. The MEP-i measurements are divided into 16 spin phases and ions are detected in 16 energy channels for each spin phase.

3. Observations

Arase was located in the morning sector (2.9–3.4 hr of magnetic local time (MLT)) and passing the magnetic equator (−2.9° to 2.9° of magnetic latitude (MLAT)) during 0040–0140 UT on 15 April 2017. Arase stayed around the apogee with the radial distance (r) of

6.0–6.1 R_E. From the decrease of the AL index shown in Figure 1a, we infer that a small substorm started at 0140 UT. Figure 1b shows the magnetic field from Arase processed with a 30–200 s band-pass filter ($\mathbf{\Delta B}$) in a mean field-aligned (MFA) coordinate system. In this system, the magnetic field averaged over a 5-min moving window is defined as the background field and gives the direction of the μ (parallel) component ($\mathbf{e}_\mu$), the direction of ϕ (azimuthal) component is defined as $\mathbf{e}_\phi = \mathbf{e}_\mu \times \mathbf{r}$, where $\mathbf{r}$ is the satellite position vector from the center of the Earth, and the direction of ν (radial) component is given by $\mathbf{e}_\nu = \mathbf{e}_\phi \times \mathbf{e}_\mu$. Four or more wave packets of Pc4 waves with a frequency of ∼13 mHz are recognized in the ΔB_μ component between 0040 UT and 0140 UT. Figures 1c–1f show the pitch angle (α) distribution of proton differential flux at energies from 56.3 keV to 109.6 keV. The flux oscillations are most clearly visible at 109.6 keV and are less significant in lower energies. Oscillations should have occurred at >109.6 keV, but this energy range was not covered by MEP-i. The energy dependence of the amplitude of flux oscillations is also found in the power spectral densities (PSDs) of log proton flux at $\alpha = 90°$ in four energy channels covering W = 56.3–109.6 keV (Figure 1g). Figure 1h shows PSDs of log proton flux at 109.6 keV in seven α bins covering 45°–135°. We find that the PSD for log proton flux around $\alpha = 90°$ is 10 times larger than that for $\alpha < 60°$ and $\alpha > 120°$. The symmetric pitch angle dependence of proton flux oscillations observed in this event indicates that the ULF waves are odd mode waves according to *Southwood & Kivelson* [1981].

After 0140 UT, toroidal or compressional waves with higher frequency were observed, but the proton flux did not oscillate. Since these waves are related to the small substorm

(Figure 1a), they are considered to be transient toroidal waves (TTWs) [*Saka et al.*, 1996; *Takahashi et al.*, 1996; *Nosé et al.*, 1998] or Pi2 waves.

To evaluate the instability condition, equation (2), we calculated each term in that equation. The radial distribution of f_{H^+} was estimated using proton measurements made during 0000–0300 UT as Arase moved radially. The coverage of L was from 5.6 to 6.1 during this interval. Figure 2a shows the radial profile of f_{H^+} evaluated at $W = 109.6$ keV and $M = 1.1$–1.3 keV/nT, which correspond to the protons showing strong oscillations at $W = 109.6$ keV and $\alpha = 90°$ at the apogee. At $L > 6$, where the Pc4 waves were observed, we find an earthward gradient of f_{H^+}. The gradient of the negative slope obtained at $L = 6.0$–6.1 is -575 s^{3}km$^{-6}/R_E$. According to equation (2), the negative energy gradient stabilizes the plasma. Therefore, another driver of destabilization is required for wave excitation. The energy dependence of f_{H^+} at the apogee was also examined (Figure 2b). The f_{H^+} averaged over the period between 0055 UT and 0115 UT is used. It seems that $\frac{\partial f_{H^+}}{\partial W}$ is negative around energy of 109.6 keV and $\frac{\partial f_{H^+}}{\partial W}$ obtained from f_{H^+} at 87.6 and 109.6 keV is -9.70 s^{3}km^{-6}/keV.

We also used an ion sounding technique to evaluate the radial gradient of f_{H^+} at the apogee. Figure 2c shows f_{H^+} at $W = 109.6$ keV and $\alpha = 90°$ as a function of time and the direction of proton guiding center relative to the spacecraft. The direction is specified using the μ-ϕ coordinates defined for the magnetic field. A clear depletion of f_{H^+} with guiding center located anti-earthward from Arase ($+\nu$) is found. Figure 2d shows the difference between the proton phase space density with anti-earthward guiding center ($f_{H^+}(+\nu)$) and earthward guiding center ($f_{H^+}(-\nu)$). The averaged value of the

difference between $f_{H^+}(+\nu)$ and $f_{H^+}(-\nu)$ during 0055–0115 UT is -130 s^{3}km^{-6}. The Larmor radius of 109.6 keV proton at the apogee is 0.087 R_E and the radial gradient of f_{H^+} is estimated to be -748 s^{3}km$^{-6}/R_E$. This is comparable to the result obtained from the radial motion of Arase. When the earthward gradient of f_{H^+} appeared during 0030–0140 UT, the Pc4 pulsations increase their amplitudes as shown in Figure 2e. This strongly suggests that the earthward gradient of f_{H^+} is related to the wave excitation.

Figure 3 shows the ground magnetometer observations of the ULF waves at European quasi-Meridional Magnetometer Array (EMMA) [*Lichtenberger et al.*, 2013]. The solid line in Figure 3a represents the magnetic field footprint of Arase traced by the T04s model [*Tsyganenko & Sitnov*, 2005] in altitude adjusted corrected geomagnetic (AACGM) coordinates. Figure 3b shows the filtered east-west component of the magnetic field (ΔB_y) observed at Kevo (KEV, $L = 6.5$), Ivalo (IVA, $L = 5.9$), Muonio (MUO, $L = 5.7$), Sodankylä (SOD, $L = 5.4$), and Ranua (RAN, $L = 4.9$). The bottom panel is the ΔB_μ component observed by Arase. Pc4 waves with a frequency of ∼12–14 mHz were observed at the ground. The Pc4 waves observed at SOD and RAN, which were near the footprint of Arase, have a wave packet structure similar to that observed by Arase. The amplitudes of the Pc4 waves observed on the ground have a peak at IVA, implying that wave source was located at $L \sim 6$. Even though the wave amplitudes (∼5 nT peak-to-peak) are slightly small compared to typical Pgs, the localization of the waves in the morning sector and around $L = 6$ is a typical feature of Pgs [e.g., *Takahashi et al.*, 2011; *Motoba et al.*, 2015].

From the delay between oscillations at the satellite and ground stations, the direction of wave propagation can be estimated. After 0055 UT, the footprint of Arase was located

to the west of the ground stations. During this period, the wave packets were observed earlier at SOD and RAN than at Arase (for example, see the wave packets observed at SOD and RAN during 0100–0110 UT and that observed by Arase during 0104–0114 UT). This suggests that the wave packets and wave phase were propagating westward. We confirmed this finding by estimating the m number from the phase difference of the Pc4 waves observed at MUO and SOD. These stations are chosen because they are separated longitudinally by 2.2° at the almost same geomagnetic latitude (64.5° and 65.3°, respectively). The m number was derived from the following equation:

$$m = \frac{\theta_{MUO} - \theta_{SOD}}{|lon_{MUO} - lon_{SOD}|}, \tag{3}$$

where $\theta_{MUO(SOD)}$ and $lon_{MUO(SOD)}$ are phase of the magnetic field oscillations and longitude of MUO (SOD) in AACGM coordinates, respectively. The ΔB_y components for MUO and SOD for the time period when Arase detected a steep earthward gradient are shown in Figure 3c. During this data period, the ΔB_y components observed at MUO and SOD have a same peak frequency at 12–14 mHz (Figure 3d), where the coherence is greater than 0.8 (Figure 3e), and the cross phase is in the small range from −108° to −113°. From the cross phase, we obtained $m \sim -49$ to -52. Westward propagation with a moderate m number is also a typical feature of Pgs [e.g., *Allan et al.*, 1983].

4. Discussion

To discuss the excitation mechanism of the Pg-like waves observed by Arase and the ground stations, we first examine the resonance signature of the drift resonance or drift-bounce resonance. The polarization of the waves observed around the magnetic equator has been discussed in previous studies. Poloidal mode waves are usually considered to be

related to the drift resonance or drift-bounce resonance; however, the radial perturbation of the magnetic field of fundamental (or odd mode) poloidal waves will be small and the compressional perturbation will become prominent near the magnetic equator as explained in *Takahashi et al.* [1992]. Since the location of Arase was near the magnetic equator and the Pc4 waves had finite amplitudes in the ΔB_μ component but not in the ΔB_ν and ΔB_ϕ components (Figure 1b), we conclude that the waves had an odd mode standing structure along the background magnetic field line. The pitch angle dependence of proton flux oscillations (Figures 1c and 1h) supports this interpretation of the mode structure. Both compressional and poloidal waves have an azimuthal electric field which can accelerate ions, thus the wave polarization is not crucial for drift or drift-bounce resonance.

Using observational parameters, we examine the resonance condition shown in equation (1). The bounce and drift angular frequencies are obtained from the following equations (4) and (5) for the dipole field [*Hamlin et al.*, 1961]:

$$\omega_b = \frac{\pi\sqrt{2W/m_p}}{2LR_E T(\alpha_{eq})}, \tag{4}$$

where m_p is mass of proton and $T(\alpha_{eq}) = 1.351 - 0.925\sin\alpha_{eq} + 0.558\sin^2\alpha_{eq} - 0.248\sin^3\alpha_{eq}$ (*Oimatsu et al.*, 2018), and

$$\omega_d = -\frac{6WLP(\alpha_{eq})}{qB_E{R_E}^2} + \frac{2\Psi_0(\mathrm{Kp})L^3\sin\phi}{B_E R_E^2} + \Omega_E, \tag{5}$$

where q is the electric charge, B_E is the magnitude of the magnetic field on the earth's surface at the magnetic equator, $P(\alpha_{eq}) = 0.340 + 0.226\sin\alpha_{eq} - 0.154\sin^2\alpha_{eq} + 0.88\sin^3\alpha_{eq}$ (*Oimatsu et al.*, 2018), $\Psi_0(\mathrm{Kp})$ is the Volland-Stern electric potential model as a function of Kp index [*Volland*, 1973; *Stern*, 1975], ϕ is the azimuthal angle eastward positive from the midnight, and Ω_E is the corotational electric field potential. As the AL index was less

than 300 nT in the event period, the dipole field well describes the inner magnetosphere. The value of B_E is obtained from the IGRF-12 model [*Thébault et al.*, 2015]. The energy of protons that resonate with the Pc4 waves is shown in Figure 4 for different values of N. Protons at $\alpha = 90°$ and Pc4 waves with a frequency of 12.7 mHz are considered in this calculation. Because the ULF waves observed in this event are considered to be odd mode waves, the drift resonance ($N = 0$) or drift-bounce resonance ($N = \pm 2$) are possible. Since the flux oscillations due to the drift-bounce resonance with odd mode waves should have a peak of amplitudes at $\alpha < 90°$ and $\alpha > 90°$ (*Yang et al.*, 2011a; *Yang et al.*, 2011b), which is not the case in the present study, only the drift resonance can explain the wave excitation. Figure 4 shows that if $N = 0$ and the resonance energy is 109.6 keV, where the proton flux was strongly oscillating, the m number is theoretically estimated to be -49. This is consistent with the m number estimated from ULF observations at the ground stations ($m \sim -50$). Therefore, the drift resonance is plausible in this event. Since 109.6 keV is the highest energy measured by MEP-i, the possibility of the drift resonance at slightly higher energies can not be excluded.

From equation (2), we determine whether wave are excited or damped through the drift resonance. According to *Southwood et al.* [1969], $\frac{dL}{dW}$ is given by $\frac{mL^2}{qR_E^2\omega B_E}$. $\frac{\partial f}{\partial L}$ was obtained from the ion sounding technique (Figures 2c and 2d), and $\frac{\partial f}{\partial W}$ was determined from the energy spectrum during 0055–0115 UT (Figure 2b). We substitute the value of m number estimated from the ground observation during 0055–0115 UT ($m \sim -50$) in equation (2). Finally, we obtain the following $\frac{df}{dW}$ at M=1.1–1.3 keV/nT and $W = 109.6$ keV:

$$\frac{df}{dW} = -9.70 + (-1.73 \times 10^{-2}) \times (-7.48 \times 10^{2}) = 3.22\ (\mathrm{s^3 km^{-6}/keV}) > 0. \qquad (6)$$

In the previous studies, only the bump-on-tail structure was considered as the energy source of Pgs [*Glassmeier et al.*, 1999; *Wright et al.*, 2001]. This result, however, suggests that the Pc4 waves were excited by the earthward gradient of f_{H^+} even if the negative slope of f_{H^+} in the energy spectrum suppress the instability. The good correspondence between the steep earthward gradient of f_{H^+} and wave excitation in Figures 2c and 2d supports this interpretation. When the spatial gradient and the energy gradient have opposite effects on the wave generation, Pgs with relatively small amplitudes may be excited as in the case of the present study.

5. Conclusions

On 15 April 2017, the Arase satellite detected a compressional magnetic field oscillation in the Pc4 band that was related to a giant pulsation observed on the ground. We examined in far more detail the oscillations of the flux of energetic (56.3–109.6 keV) protons than reported previously [*Glassmeier et al.*, 1999; *Thompson & Kivelson*, 2001; *Motoba et al.*, 2015]. We found evidence that the waves had an odd mode standing structure along the background magnetic field and that the waves were in drift resonance with ∼110 keV protons. The Arase satellite also detected an earthward gradient of f_{H^+}. Several previous studies considered the bump-on-tail structure in energy spectrum of f_{H^+} as an energy source of Pgs. However, the Pc4 waves examined in this study are excited by the steep earthward gradient of f_{H^+}. We suggest that the spatial distribution of the phase space density also plays an important role in the exicitation of Pgs.

Acknowledgments. The EMMA magnetometer data were provided by M. Vellante and B. Heilig, the PIs of the EMMA. We thank the institutes who maintain EMMA

stations used for this study: the Finnish Meteorological Institute (Finland), Sodankylä Geophysical Observatory of the University of Oulu (Finland). Science data of the Arase (ERG) satellite were obtained from the ERG Science Center operated by ISAS/JAXA and ISEE/Nagoya University (https://ergsc.isee.nagoya-u.ac.jp/index.shtml.en). The present study analyzed the MGF v01.00 data and the MEP-i v01_00 data. The AL index was provided by the World Data Center for Geomagnetism, Kyoto. The Kp index was provided by GeoForschungsZentrum (GFZ) Potsdam, Germany. The geomagnetic field by the IGRF-12 model is calculated by the World Data Center for Geomagnetism, Kyoto (http://wdc.kugi.kyoto-u.ac.jp/igrf/point/index-j.html). This study was supported by Japan Society for the Promotion of Science (JSPS), Grant-in-Aid for Scientific Research (B) (grant 16H04057), Challenging Research (Pioneering) (17K18804), and Grant-in-Aid for Specially Promoted Research (16H06286). KT was supported by NASA grant NNX14AB97G. YM was supported by JSPS, Grant-in-Aid for Scientific Research on Innovative Areas (Research in a proposed research area) (grant 15H05815).

References

Allan, W., Poulter, E. M., Glassmeier, K., & Nielson, E. (1983). Ground magnetometer detection of a large-M Pc 5 pulsation observed with the STARE radar. *Journal of Geophysical Research: Space Physics*, *88*(A1), 183–188. https://doi.org/10.1029/JA088iA01p00183

Brekke, A., Feder, T., & Berger, S. (1987). Pc4 giant pulsations recorded in Tromsø, 1929–1985. *Journal of Atmospheric and Terrestrial Physics*, *49*(10), 1027–1032. https://doi.org/10.1016/0021-9169(87)90109-7

Chisham, G. (1996). Giant pulsations: An explanation for their rarity and occurrence during geomagnetically quiet times. *Journal of Geophysical Research: Space Physics*, *101*(A11), 24,755–24,763. https://doi.org/10.1029/96JA02540

Chisham, G., & Orr, D. (1991). Statistical studies of giant pulsations (Pgs): harmonic mode. *Planetary and Space Science*, *39*(7), 999–1006. https://doi.org/10.1016/0032-0633(91)90105-J

Chisham, G., & Orr, D. (1994). The association between giant pulsations (Pgs) and the auroral oval. *Annales Geophysicae*, *12*(7), 649–654. https://doi.org/10.1007/s00585-994-0649-4

Chisham, G., Mann, I. R., & Orr, D. (1997). A statistical study of giant pulsation latitudinal polarization and amplitude variation. *Journal of Geophysical Research: Space Physics*, *102*(A5), 9619–9629. https://doi.org/10.1029/97JA00325

Dai, L., Takahashi, K., Wygant, J. R., Chen, L., Bonnell, J., Cattell, C., et al. (2013). Excitation of poloidal standing Alfvén waves through drift reso-

nance wave-particle interaction. *Geophysical Research Letters*, *40*(16), 4127–4132. https://doi.org/10.1002/grl.50800

Glassmeier, K.-H. (1980). Magnetometer array observations of a giant pulsation event. *Journal of Geophysics*, *48*(3), 127–138.

Glassmeier, K.-H., Buchert, S., Motschmann, U., Korth, A., & Pedersen, A. (1999). Concerning the generation of geomagnetic giant pulsations by drift-bounce resonance ring current instabilities. *Annales Geophysicae*, *17*(3), 338–350. https://doi.org/10.1007/s00585-999-0338-4

Hamlin, D. A., Karplus, R., Vik, R. C., & Watson, K. M. (1961). Mirror and azimuthal drift frequencies for geomagnetically trapped particles. *Journal of Geophysical Research*, *66*(1), 1–4. https://doi.org/10.1029/JZ066i001p00001

Hughes, W. J., & Southwood, D. J. (1976). The screening of micropulsation signals by the atmosphere and ionosphere. *Journal of Geophysical Research*, *81*(19), 3234–3240. https://doi.org/10.1029/JA081i019p03234

Lichtenberger, J., Clilverd, M. A., Heilig, B., Vellante, M., Manninen, J., Rodger, C. J., et al. (2013). The plasmasphere during a space weather event: first results from the PLASMON project. *J. Space Weather Space Clim.*, *3*, A23. https://doi.org/10.1051/swsc/2013045

Matsuoka, A., Teramoto, M., Nomura, R., Nosé, M., Fujimoto, A., Tanaka, et al. (2018). The ARASE (ERG) magnetic field investigation. *Earth, Planets and Space*, *70*(1), 43. https://doi.org/10.1186/s40623-018-0800-1

McIlwain, C. E. (1961). Coordinates for mapping the distribution of magnetically trapped particles. *Journal of Geophysical Research*, *66*(11), 3681–3691. https://doi.org/10.1029/JZ066i011p03681

Min, K., Takahashi, K., Ukhorskiy, A. Y., Manweiler, J. W., Spence, H. E., Singer, J., et al. (2017). Second harmonic poloidal waves observed by Van Allen Probes in the dusk-midnight sector. *Journal of Geophysical Research: Space Physics*, *122*(3), 3013–3039. 2016JA023770. https://doi.org/10.1002/2016JA023770

Miyoshi, Y., Shinohara, I., Takashima, T., Asamura, K., Higashio, N., Mitani, T., et al. (2018). Geospace exploration project ERG. *Earth, Planets and Space*, *70*, XXX-XXX. https://doi.org/10.1186/s40623-018-0862-0

Motoba, T., Takahashi, K., Rodriguez, J. V., & Russell, C. T. (2015). Giant pulsations on the afternoonside: Geostationary satellite and ground observations. *Journal of Geophysical Research: Space Physics*, *120*(10), 8350–8367. 2015JA021592. https://doi.org/10.1002/2015JA021592

Nosé, M., Iyemori, T., Nakabe, S., Nagai, T., Matsumoto, H., & Goka, T. (1998). ULF pulsations observed by the ETS-VI satellite: Substorm associated azimuthal Pc 4 pulsations on the nightside. *Earth, Planets and Space*, *50*(1), 63–80. https://doi.org/10.1186/BF03352087

Oimatsu, S., Nosé, M., Takahashi, K., Yamamoto, K., Keika, K., Kletzing, C. A., et al. (2018). Van Allen Probes observations of drift-bounce resonance and energy transfer between energetic ring current protons and poloidal Pc4 wave. *Journal of Geophysical Research: Space Physics*, *123*. https://doi.org/10.1029/2017JA025087

Ozeke, L. G., & Mann, I. R. (2001). Modeling the properties of high-m Alfvén waves driven by the drift-bounce resonance mechanism. *Journal of Geophysical Research: Space Physics*, *106*(A8), 15,583–15,597. https://doi.org/10.1029/2000JA000393

Saka, O., Watanabe, O., & Baker, D. N. (1996). A possible driving source for tran-sient field line oscillations in the postmidnight sector at geosynchronous altitudes. *J. Geophys. Res.*, *101*. https://doi.org/10.1029/96JA02039

Southwood, D., Dungey, J., & Etherington, R. (1969). Bounce resonant interaction between pulsations and trapped particles. *Planetary and Space Science*, *17*(3), 349–361. https://doi.org/10.1016/0032-0633(69)90068-3

Southwood, D. J., & Kivelson, M. G. (1981). Charged particle behavior in low-frequency geomagnetic pulsations 1. Transverse waves. *Journal of Geophysical Research: Space Physics*, *86*(A7), 5643–5655. https://doi.org/10.1029/JA086iA07p05643

Stern, D. P. (1975). The motion of a proton in the equatorial magnetosphere. *Journal of Geophysical Research*, *80*(4), 595–599. https://doi.org/10.1029/JA080i004p00595

Su, S. Y., Konradi, A., & Fritz, T. A. (1977). On propagation direction of ring current proton ULF waves observed by ATS 6 at 6.6 R_E. *Journal of Geophysical Research*, *82*(13), 1859–1868. https://doi.org/10.1029/JA082i013p01859

Sucksdorff, E. (1939). Giant pulsations recorded at Sodankylä during 1914–1938. *Terrestrial Magnetism and Atmospheric Electricity*, *44*(2), 157–170. https://doi.org/10.1029/TE044i002p00157

Takahashi, K., McEntire, R. W., Lui, A. T. Y., & Potemra, T. A. (1990). Ion flux oscillations associated with a radially polarized transverse Pc 5 magnetic

pulsation. *Journal of Geophysical Research: Space Physics*, *95*(A4), 3717–3731. https://doi.org/10.1029/JA095iA04p03717

Takahashi, K., Sato, N., Warnecke, J., Lühr, H., Spence, H. E., & Tonegawa, Y. (1992). On the standing wave mode of giant pulsations. *Journal of Geophysical Research: Space Physics*, *97*(A7), 10,717–10,732. https://doi.org/10.1029/92JA00382

Takahashi, K., Anderson, B. J., & Ohtani, S.-i. (1996). Multisatellite study of nightside transient toroidal waves. *Journal of Geophysical Research: Space Physics*, *101*(A11), 24,815–24,825. https://doi.org/10.1029/96JA02045

Takahashi, K., Glassmeier, K.-H., Angelopoulos, V., Bonnell, J., Nishimura, Y., Singer, H. J., & Russell, C. T. (2011). Multisatellite observations of a giant pulsation event. *Journal of Geophysical Research: Space Physics*, *116*(A11), A11223. https://doi.org/10.1029/2011JA016955

Takahashi, K., Oimatsu, S., Nosé, M., Min, K., Claudepierre, S. G., Chan, A., et al. (2018). Van Allen Probes observations of second harmonic poloidal standing Alfvén waves. *Journal of Geophysical Research: Space Physics*, *123*, 611–637. https://doi.org/10.1002/2017JA024869

Thébault, E., Finlay, C. C., Beggan, C. D., Alken, P., Aubert, J., Barrois, O., et al. (2015). International geomagnetic reference field: the 12th generation. *Earth, Planets and Space*, *67*(1), 79. https://doi.org/10.1186/s40623-015-0228-9

Thompson, S. M., & Kivelson, M. G. (2001). New evidence for the origin of giant pulsations. *Journal of Geophysical Research: Space Physics*, *106*(A10), 21,237–21,253. https://doi.org/10.1029/2001JA000026

Tsyganenko, N. A., & Sitnov, M. I. (2005). Modeling the dynamics of the inner magnetosphere during strong geomagnetic storms. *Journal of Geophysical Research: Space Physics*, *110*(A3), A03208. https://doi.org/10.1029/2004JA010798

Volland, H. (1973). A semiempirical model of large-scale magnetospheric electric fields. *Journal of Geophysical Research*, *78*(1), 171–180. https://doi.org/10.1029/JA078i001p00171

Wright, D. M., Yeoman, T. K., Rae, I. J., Storey, J., Stockton-Chalk, A. B., Roeder, J. L., & Trattner, K. J. (2001). Ground-based and Polar spacecraft observations of a giant (Pg) pulsation and its associated source mechanism. *Journal of Geophysical Research: Space Physics*, *106*(A6), 10,837–10,852. https://doi.org/10.1029/2001JA900022

Yang, B., Zong, Q., Fu, S. Y., Li, X., Korth, A., Fu, et al. (2011a). The role of ULF waves interacting with oxygen ions at the outer ring current during storm times. *Journal of Geophysical Research: Space Physics*, *116*(A1). https://doi.org/10.1029/2010JA015683

Yang, B., Zong, Q., Fu, S. Y., Takahashi, K., Li, X., Wang, et al. (2011b). Pitch angle evolutions of oxygen ions driven by storm time ULF poloidal standing waves. *Journal of Geophysical Research: Space Physics*, *116*(A3). https://doi.org/10.1029/2010JA016047

Yokota, S., Kasahara, S., Mitani, T., Asamura, K., Hirahara, M., Takashima, T., et al. (2017). Medium-energy particle experiments–ion mass analyzer (MEP-i) onboard ERG (Arase). *Earth, Planets and Space*, *69*(1), 172. https://doi.org/10.1186/s40623-017-0754-8

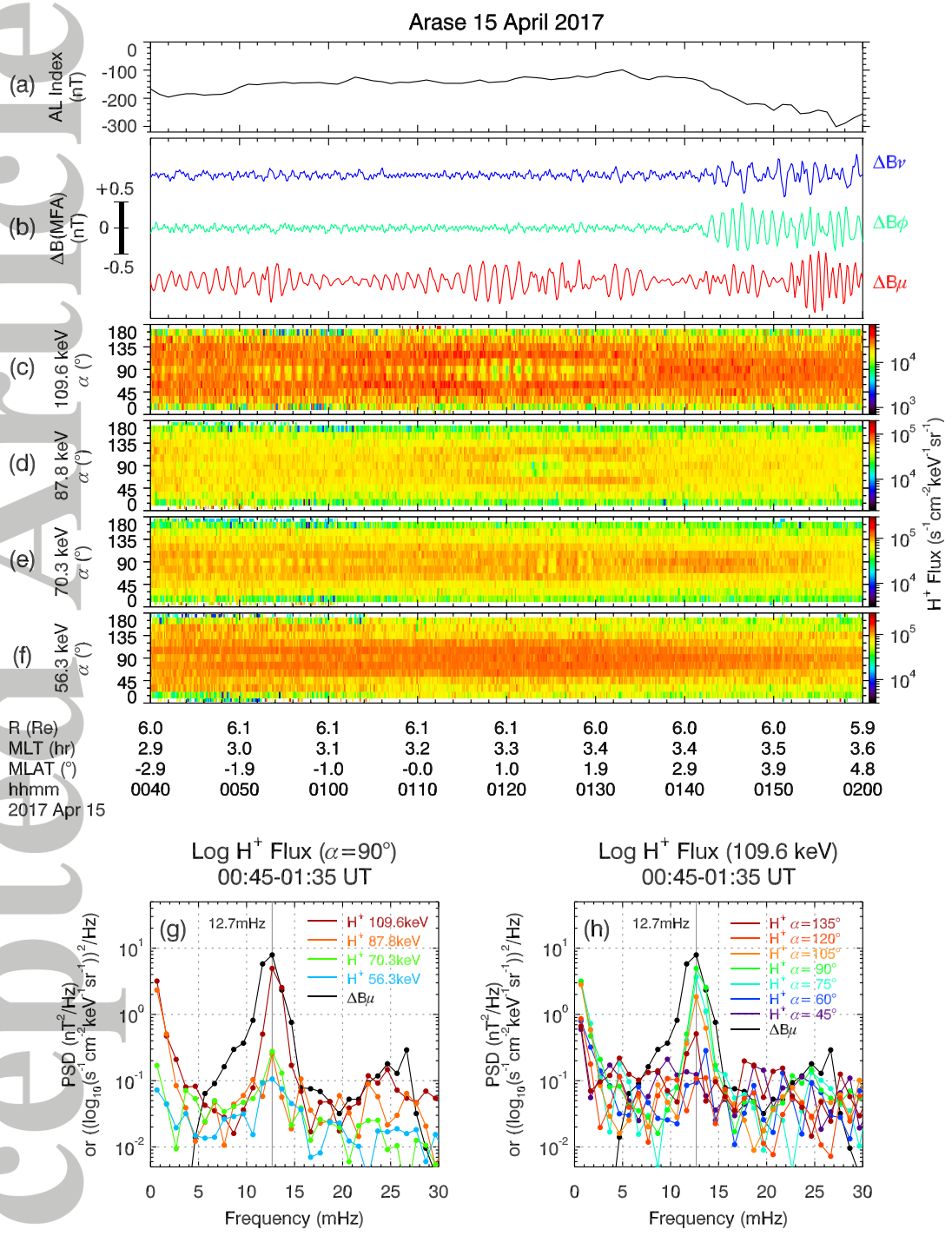

Figure 1. (a) The AL index. (b) The magnetic field observed by Arase in MFA coordinates. The blue line represents radial component, the green line represents azimuthal component, and the red line represents parallel component. (c–f) The pitch angle distribution of proton differential flux at energies of 109.6, 87.8, 70.3, and 56.3 keV. (g) PSDs for ΔB_μ component and log proton flux at $\alpha = 90°$ and $W = 56.3$–109.6 keV. (h) PSDs for ΔB_μ component and proton flux at $W = 109.6$ keV and $\alpha = 45°$–$145°$.

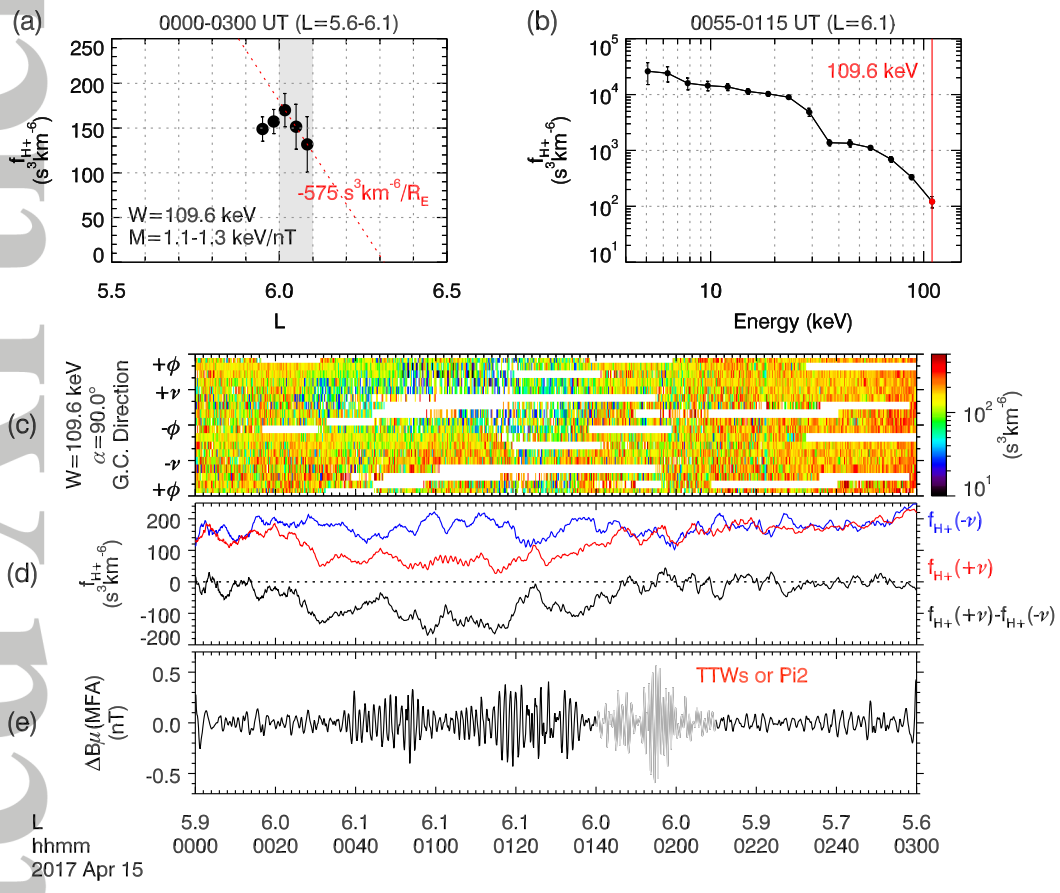

Figure 2. (a) The radial profile of f_{H^+} at W = 109.8 keV and M = 1.1–1.3 keV/nT. The standard deviation is shown for each point. (b) The energy dependence of f_{H^+} near the apogee. (c) f_{H^+} obtained from an ion sounding technique as a function of time and the direction of proton guiding center relative to the spacecraft. (d) 3-min running average of $f_{H^+}(+\nu)$ (red line) and $f_{H^+}(-\nu)$ (blue line), and the difference between $f_{H^+}(+\nu)$ and $f_{H^+}(-\nu)$ (black line). (e) ΔB_μ component observed by Arase. The TTWs or Pi2 wave oscillations are colored in gray.

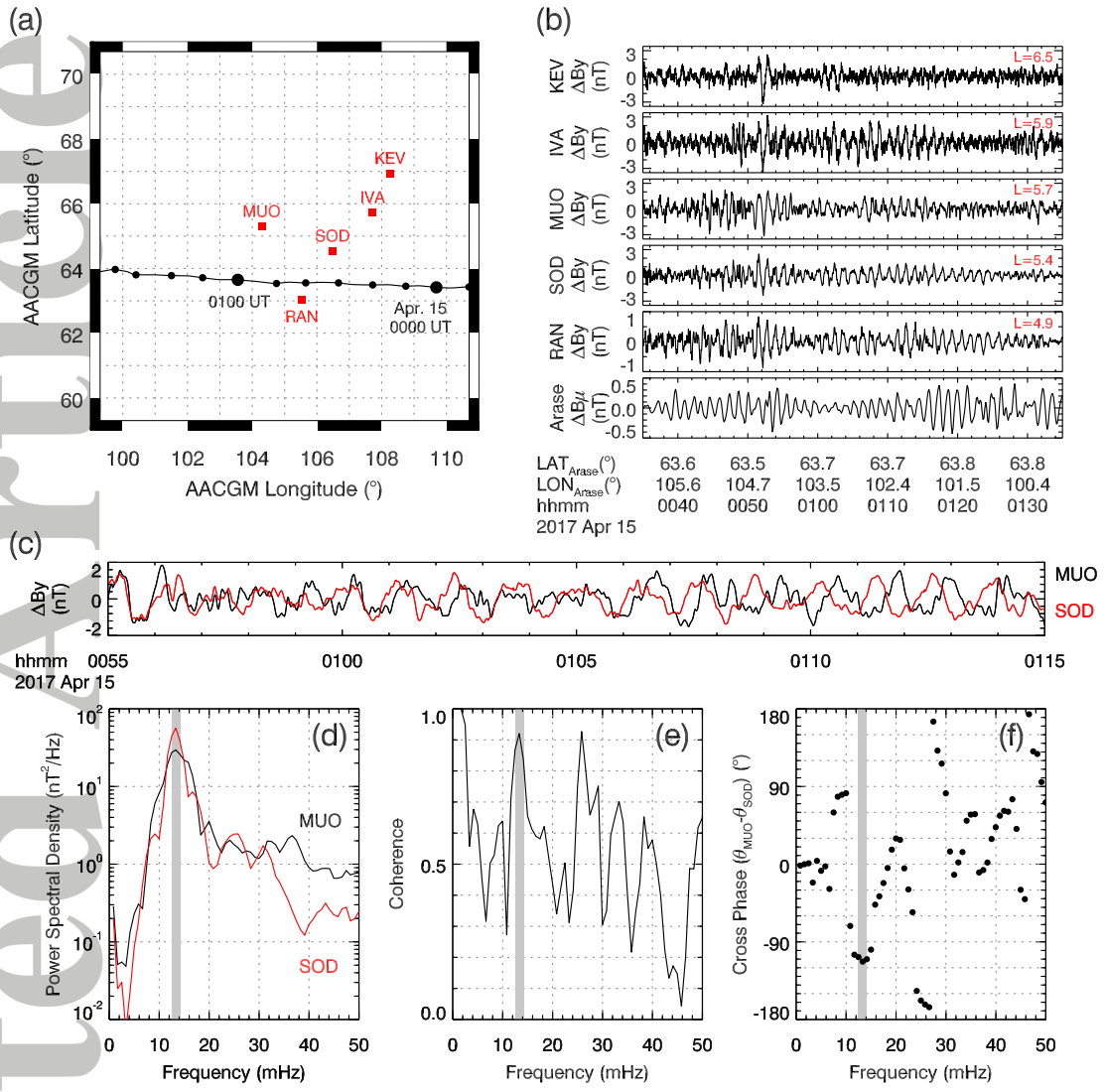

Figure 3. (a) Locations of the Arase's magnetic field footprint and EMMA magnetometer stations in AACGM coordinates. The large solid circles indicate locations of Arase every one hour. The small solid circles are marked every 10 minutes. (b) ΔB_y component observed at the magnetometer stations. The background field is removed by a Savitzky-Golay filter with a window width of 200 s. (c) ΔB_y components observed at MUO (black line) and SOD (red line) during 0055–0115 UT. (d–f) Power spectra, coherence, and cross phase estimated from the data shown in (c). The spectral peaks are highlighted by shading in gray. Only the data points with coherence greater than 0.8 are shown in the cross phase.

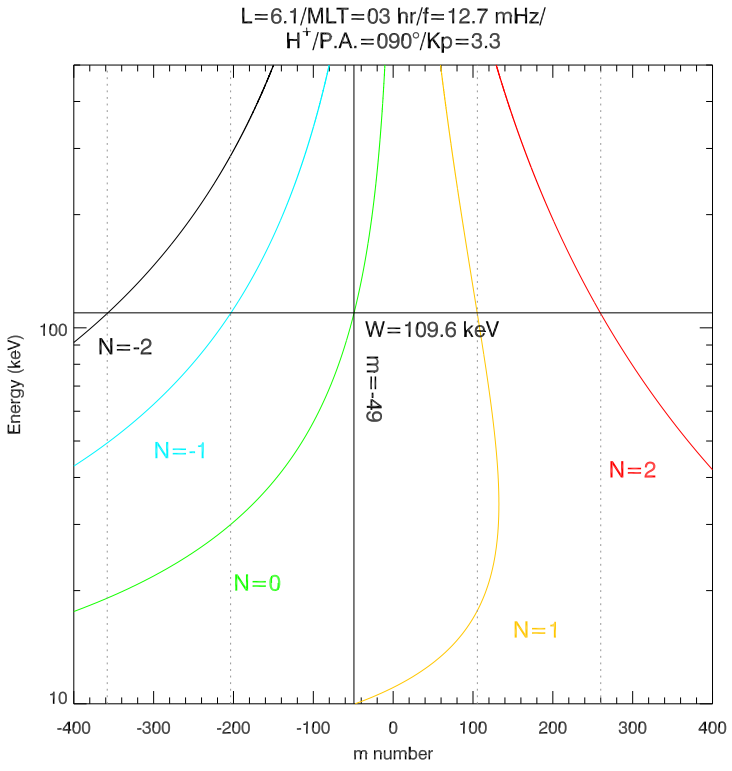

Figure 4. Energy of protons that are in resonance with ULF waves at $L = 6.1$ as a function of the m number of the waves, shown for a wave frequency of 12.7 mHz and the equatorial pitch angle of 90°.